Valence electronic states related to Mn^{2+} at $La_{0.7}Sr_{0.3}MnO_3$ surfaces characterized by resonant photoemission

M. P. de Jong,[1] I. Bergenti,[2] W. Osikowicz,[1] R. Friedlein,[1] V. A. Dediu,[2] C. Taliani,[2] and W. R. Salaneck[1]
[1]*Department of Physics, IFM, Linköping University, S-581 83 Linköping, Sweden*
[2]*ISMN-CNR, via Gobetti 101, 40129 Bologna, Italy*
(Received 2 November 2005; revised manuscript received 15 December 2005; published 14 February 2006)

Nonferromagnetic Mn^{2+} ions can be readily formed at the surface of half metallic $La_{0.7}Sr_{0.3}MnO_3$ manganite as demonstrated by deoxygenating surface treatments. The $3d^5$ contribution of these Mn^{2+} ions to the valence-band electronic structure has been characterized using Mn($2p$) to $3d$ resonant photoemission measurements. The Mn^{2+} related $3d$ electrons were found to be stabilized by about 2 eV with respect to the mixed-valence $3d$ states, indicating their strong localization. Active participation of Mn^{2+} states in both spin and charge conductivity processes is therefore excluded. A two-channel picture, including independent Mn^{3+}/Mn^{4+} and Mn^{2+} channels, emerges from detailed data analysis. Reversible Mn^{2+} formation and straightforward oxygen annealing effects point to a direct bonding between Mn^{2+} and oxygen vacancies that are most probably created at preexisting structural defects. The t_{2g} and e_g states of the mixed valence Mn^{3+}/Mn^{4+} ions remain unaffected as the Mn^{2+} content increases, indicating a robust Mn^{3+}/Mn^{4+} channel independent of structural defects.

DOI: 10.1103/PhysRevB.73.052403 PACS number(s): 75.47.Lx, 78.70.Dm, 73.20.Hb

The high spin polarization near the Fermi level in mixed-valence manganites, which reaches 100% well below the Curie temperature T_C,[1] makes this class of materials very attractive as spin injecting contacts in spintronics devices. For truly half metallic systems, the conductivity mismatch limitation[2] that generally suppresses spin injection at ferromagnetic metal-semiconductor contacts no longer holds. Indeed, considerable spin injection has been demonstrated for, e.g., hybrid inorganic or organic heterostructures, consisting of manganites and organic molecular semiconductors.[3,4]

Many issues concerning the optimization of the interfacial electronic and magnetic properties are related to the manganite surfaces, for which the characteristics deviate markedly from the bulk and depend sensitively on the preparation conditions. In compounds of the form $R_xA_{1-x}MnO_{3+\delta}$, where R is a trivalent rare-earth cation and A is a divalent alkaline-earth cation, surface segregation of alkaline-earth species is common,[5–7] and the (surface) oxygen content depends critically on the film growth parameters and post-deposition treatments. In turn, the oxygen content affects the nominal valence of the Mn ions, which is a key parameter in the interplay between ferromagnetic ordering, associated with delocalized electronic states, and charge ordering related to the localization of states. Traditionally, the Mn valence is described as a mixture of 3+ and 4+, in accordance with the qualitative model of double exchange[8] as the mechanism behind the correlation of electron delocalization and ferromagnetic coupling. Such a purely ionic picture is, however, an oversimplification of reality, and the detailed description of the Mn valence in manganites is under intense debate. For $Nd_{0.5}Sr_{0.5}MnO_3$, which is commonly accepted to exhibit charge and Mn($3d$) orbital ordering, it has been shown recently that, although there are indeed two different Mn sites, these are mainly characterized by different geometries of the surrounding oxygen octahedra and show a rather small charge disproportionation of $Mn^{+3.42}$-$Mn^{+3.58}$.[9] A small charge modulation of $\sim$0.15 has also been obtained by theoretical modeling of manganites with composition $R_xA_{1-x}MnO_3$, $x>0.5$, where the charge is modulated along diagonals of the lattice with a periodicity that scales inversely with x.[10] Furthermore, the coexistence between charge ordering and ferromagnetism in $La_{0.5}Ca_{0.5}MnO_3$ (Ref. 11) was recently explained within the framework of a phenomenological Ginzburg-Landau theory, where the charge modulation is described in terms of delocalized charge density waves rather than by charges localized on specific Mn sites.[12]

At the surface, the situation is further complicated by the obvious termination of the periodicity, possibly the loss of octahedral symmetry around the Mn ions,[13] a higher concentration of defects such as oxygen vacancies,[14] and the aforementioned segregation of alkaline-earth species. Recently, we showed that $La_{0.7}Sr_{0.3}MnO_3$ (LSMO) surfaces contain Mn^{2+} by means of surface sensitive x-ray-absorption spectroscopy (XAS) of the Mn $L_{2,3}$ edge, and photoelectron spectroscopy (PES) of the Mn($3s$) exchange splitting.[15] The Mn^{2+} ions were reversibly created (annihilated) at the surface upon deoxygenation (oxygenation) treatments, strongly suggesting a correlation between Mn^{2+} ion formation and oxygen vacancies. The XAS spectral profile associated with the Mn^{2+} ions did not display a magnetic circular dichroism effect, indicating that no ferromagnetic ordering of spins at the Mn^{2+} sites exists. Consequently, the spin injection efficiency in devices could be severely compromised, depending on to what extent the $3d$ states of the Mn^{2+} ions contribute to the injected current.

In order to characterize the Mn^{2+} contribution to the valence electronic structure, we have carried out resonant photoemission (RPE) measurements using the sharp $2p-3d$ resonance of the Mn^{2+} ion. The measurements were carried out at beamline D1011 at the MAX-Laboratory for Synchrotron Radiation Research in Lund, Sweden. The end station contains a Scienta ESCA200 hemispherical electron analyzer, and a purpose built microchannel plate (MCP)

 ©2006 The American Physical Society

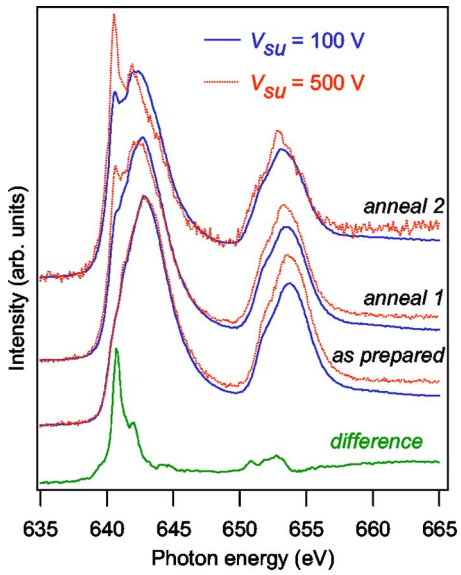

FIG. 1. (Color online) XAS Mn L-edge spectra of LSMO on $SrTiO_3$, for various post-deposition treatments, recorded with different surface sensitivity as explained in the text. The difference curve (bottom) was obtained by subtracting the weighted "as-prepared" spectrum from the "anneal 2" spectrum (V_{SU}=100 V in both cases).

electron-yield detector. PES and RPE spectra were recorded with the electron emission direction along the sample normal, for which the angle of incidence of the photon beam was 50°. The same experimental geometry has been used for the XAS measurements. Both the photon linewidth and the energy resolution of the electron analyzer were kept well below 100 meV.

Figure 1 shows XAS Mn $L_{2,3}$-edge spectra for a thin LSMO film on $SrTiO_3$, obtained from as-prepared films[15] and after two cycles (anneal 1, anneal 2) of annealing at 450°C for about 5 min in ultrahigh vacuum. The spectra were obtained using either a 100-V or 500-V secondary-electron suppression voltage V_{SU}, resulting in probing depths of 50–100 Å and about 10 Å, respectively.[16] As described previously, annealing results in oxygen loss, which in turn induces Mn^{2+} ions at the surface.[15] These Mn^{2+} ions produce a distinct XAS fingerprint, which appears in the raw data as a sharp structure at about 640 eVand is clearly visible upon taking the difference between the XAS spectra of the annealed and as-prepared case (Fig. 1, bottom curve).[15] The increased Mn^{2+}-related signal in the surface sensitive spectrum confirms that the Mn^{2+} ions are confined to the surface region.

By comparing RPE spectra taken at different photon energies within the $2p-3d$ resonance obtained after different deoxygenation treatments, the Mn^{2+} contribution to the valence electronic structure becomes apparent. Figure 2 shows off-resonance PES spectra, recorded at $h\nu$=636.6 eV, plus RPE spectra recorded at the maxima of (i) the surface Mn^{2+} XAS peak ($h\nu$=640.9 eV) and (ii) the XAS peak associated with bulk, mixed-valence Mn ($h\nu$=643.0 eV). The photon energies used to record the RPE spectra are indicated by the arrows in the XAS spectra shown in the left-hand panel. In

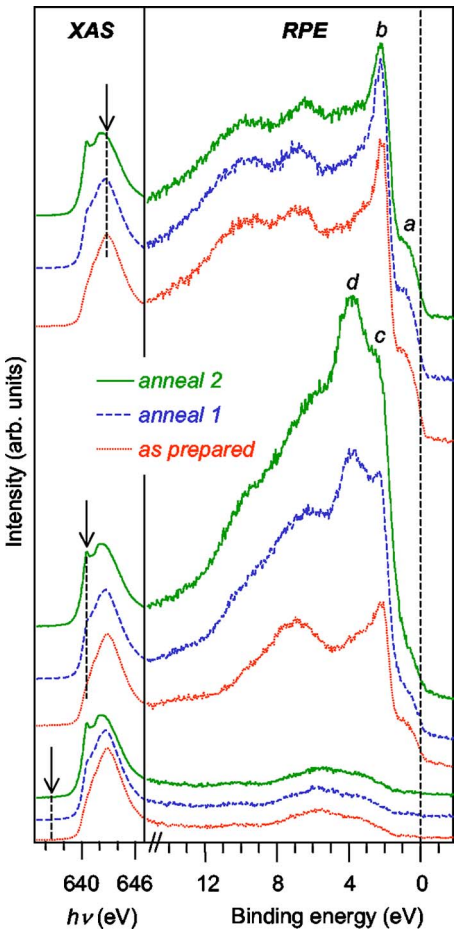

FIG. 2. (Color online) RPE, PES, and XAS spectra of LSMO on $SrTiO_3$ for various post-deposition treatments. The PES and RPE spectra (right) are grouped according to the photon energies indicated by arrows in the corresponding XAS spectra (left). For the as-prepared film, two strongly resonating Mn($3d$) derived features can be observed in the RPE spectra, corresponding to the e_g (labeled a) and t_{2g} (labeled b) states of the mixed-valence Mn ions.[18,19] After annealing, two new peaks appear, labeled c and d, due to the e_g and t_{2g} states of the Mn^{2+} ion, respectively.

order to show the relationship between the XAS and PES or RPE spectra recorded after the various treatments, the spectra are joined at the intersect between the two panels in Fig. 2 (note that the same XAS spectra are shown for each group of PES/RPE spectra measured with a certain photon energy). Let us first discuss the spectra obtained for the as-prepared sample (dotted lines). In the off-resonance PES spectrum, the main spectral weight stems from O($2p$) related photoelectron emission[17] giving rise to a broad signal between 2- and 8-eV binding energy. In the $2p$ to $3d$ resonance, Mn($3d$) states are strongly enhanced, and two clear structures corresponding to the e_g (labeled a) and t_{2g} (labeled b) states of the Mn ions[18,19] can be observed. The e_g-related feature a has a significant spectral weight at the Fermi level, confirming the presence of a metallic phase. Although no surface cleaning treatment (annealing) was carried out, the RPE spectra are very similar to those obtained for *in situ* prepared LSMO,[19] showing that, as expected, surface contamination has little effect on the Mn($3d$)-derived local electronic structure. Due to the strong

hybridization between the Mn($3d$) and O($2p$) orbitals, resonant enhancement of states with mainly O($2p$) character is observed as well. The resonant process can thus be described in terms of transitions of the form $3d^n \rightarrow \underline{c}3d^{n+1} \rightarrow 3d^{n-1} + e^-$ and $3d^n \rightarrow \underline{c}3d^{n+1} \rightarrow 3d^n\underline{L} + e^-$, where $\underline{c}$ is a Mn($2p$) core hole and $\underline{L}$ is a ligand hole. The peak at about 7 eV binding energy corresponds to a $3d^n\underline{L} + e^-$ final state, with the hole located in a σ bonding orbital of mixed O($2p$) and Mn($3d$) character,[17,20] while π bonding orbitals contribute to the intensity between 5 and 2 eV, close to the t_{2g} peak.[21] The peak at about 10-eV binding energy in the RPE spectrum recorded at the maximum of the Mn $L_{2,3}$ edge ($h\nu$=643.0 eV) is due to an Auger-like spectator decay process,[20] as can be concluded from its linear dispersion with the photon energy in previously published data.[19] In addition, the spectra may contain weak contributions from additional $3d^n\underline{L} + e^-$ final states, so-called satellites, in the binding energy region above 10 eV.[17]

We now address the changes observed in the RPE and PES spectra that occur upon deoxygenation by annealing treatments, related to the growth of the Mn^{2+} signal in the XAS spectra. In the off-resonance PES spectra, mainly reflecting states with O($2p$) character, no significant changes can be observed, indicating that the O($2p$) derived electronic structure remains largely unaffected by the creation of oxygen vacancies. For RPE spectra recorded at $h\nu$=643.0 eV, i.e., in the XAS maximum associated with bulk, mixed-valence Mn, changes are again minor: only a small increase of the spectral intensity between 6 and 3 eV is observed. This is because at $h\nu$=643.0 eV the XAS signal for Mn^{2+} ions is very low compared to the Mn^{3+}/Mn^{4+} peak (see Fig. 1). Consequently, the contribution of Mn^{2+} ions to the RPE spectra is small. If the photon energy is tuned to the sharp Mn^{2+} XAS peak ($h\nu$=640.9 eV), however, strong changes in the Mn $2p-3d$ RPE spectra become visible. Additional, Mn^{2+}-derived de-excitation channels originate from $3d^5 \rightarrow \underline{c}3d^6 \rightarrow 3d^4 + e^-$ transitions and produce two new peaks, labeled c and d, due to the e_g and t_{2g} states of the Mn^{2+} ion, respectively. Clearly, the $3d$ levels of the Mn^{2+} ion are stabilized by about 2 eV as compared to those of the mixed-valence Mn species, consistent with a strongly localized character of the Mn^{2+} valence electrons. Therefore Mn^{2+} electrons will not contribute directly to charge injection across the interface. This is a very important result concerning spin injection in spintronic devices. Although spin scattering at Mn^{2+} sites may decrease the spin polarization to some extent, the presence of Mn^{2+} at the surface, although not desirable, will not form a major obstacle for spin injection experiments.

Even though it is clear that the formation of Mn^{2+} ions at the surface is related to the creation of oxygen vacancies, the exact mechanism by which these vacancies are formed remains somewhat ambiguous and deserves further attention. A charge disproportionation reaction $Mn^{3+} + Mn^{3+} \rightarrow Mn^{2+} + Mn^{4+}$ ($3d^4 3d^4 \rightarrow 3d^5 3d^3$) has been proposed for bulk $La_{1-x}Ca_xMnO_3$ in order to explain the exceptionally low Seebeck coefficient determined from thermoelectric power measurements.[22] The $3d^4 3d^4$ and $3d^5 3d^3$ states should be nearly degenerate, with static Jahn-Teller distortion favoring the $3d^4 3d^4$ configuration due to the large size of the Mn^{2+} ion (30% larger than Mn^{3+}) while exchange interactions could stabilize $3d^5 3d^3$ states. No evidence for Mn^{2+}, however, has been found either with electron spin resonance[23] or x-ray emission spectroscopy,[24] which are both bulk sensitive techniques, in principle ruling out this scenario for the bulk. Still, such a mechanism cannot *a priori* be excluded to occur at the surface, where the energy needed to displace surrounding oxygen atoms is much smaller, effectively stabilizing the $3d^5 3d^3$ state. A small reduction in the near surface oxygen content, as is induced in our annealing experiments, might then drive the charge disproportionation reaction. However, if $3d^5 3d^3$ states would be formed, the occupation of the frontier e_g band would decrease since the Mn^{2+} $3d$ electrons form localized bands and the Mn^{4+} ions have no electrons in the e_g states.

Conversely, our experiments show that the e_g related feature a in Fig. 2 remains unaffected by the annealing treatments. This suggests that the Mn^{2+} ions are related to localized oxygen vacancies, most probably formed by the removal of oxygen from some structural defects intrinsically present in the films. It is well known that oxygen vacancies can be easily formed[14,25] and cured[26] by annealing treatments using varying oxygen partial pressures, in agreement with our observation of the reversible creation of Mn^{2+} species.[15] The crystal field strength $10Dq$ at Mn^{2+} sites is estimated as 1.6–1.7 eV from the energetic separation of peaks c and d in Fig. 2 assigned to Mn^{2+} e_g and t_{2g} states. For such a large value of $10Dq$, in case of octahedral symmetry (O_h), the multiplet structure of the Mn^{2+} L-edge XAS spectrum is expected to exhibit a clear peak splitoff from the main L_3 peak towards lower photon energy.[27,28] In contrast, only a weak shoulder can be observed at about 639 eV in the difference spectrum in Fig. 1. This observation might be related to a reduction of the symmetry from O_h to C_{4v}, which would result from direct bonding between Mn^{2+} ions and oxygen vacancies.

In conclusion, we have shown that the controversial behavior of the Mn valence in LSMO is further complicated at the surface by the formation of Mn^{2+} related to oxygen deficiency. RPE measurements show that the corresponding $3d$ electrons are strongly stabilized and thus localized, meaning that they will not participate actively in spin injection. The Mn^{2+} ions appear to be bonded to oxygen vacancies that are most probably created at preexisting structural defects upon annealing, while alternative charge disproportionation of $3d^4 3d^4$ to $3d^5 3d^2$ states is unlikely to occur even at the surface. This is in agreement with the observation that both the t_{2g} and $e_g$states of the mixed valence Mn^{3+}/Mn^{4+} ions remain unaffected as the Mn^{2+} content increases, indicating a robust Mn^{3+}/Mn^{4+} channel independent of structural defects.

[1] J. H. Park, E. Vescovo, H. J. Kim, C. Kwon, R. Ramesh, and T. Venkatesan, Nature (London) **392**, 794 (1998).
[2] G. Schmidt, D. Ferrand, L. W. Molenkamp, A. T. Filip, and B. J. vanWees, Phys. Rev. B **62**, R4790 (2000).
[3] V. Dediu, M. Murgia, F. C. Matacotta, C. Taliani, and S. Barbanera, Solid State Commun. **122**, 181 (2002).
[4] Z. H. Xiong, D. Wu, Z. V. Vardeny, and J. Shi, Nature (London) **427**, 821 (2004).
[5] H. Dulli, P. A. Dowben, S. -H. Liou, and E. W. Plummer, Phys. Rev. B **62**, R14629 (2000).
[6] J. Choi, J. Zhang, S. -H. Liou, P. A. Dowben, and E. W. Plummer, Phys. Rev. B **59**, 13453 (1999).
[7] M. P. de Jong, V. A. Dediu, C. Taliani, and W. R. Salaneck, J. Appl. Phys. **94**, 7292 (2003).
[8] C. Zener, Phys. Rev. **82**, 403 (1951).
[9] J. Herrero-Martín, J. García, G. Subías, J. Blasco, and M. Concepción Sánchez, Phys. Rev. B **70**, 024408 (2004).
[10] L. Brey, Phys. Rev. Lett. **92**, 127202 (2004).
[11] J. C. Loudon, N. D. Mathur, and P. A. Midgley, Nature (London) **420**, 797 (2002).
[12] G. C. Milward, M. J. Calderon, and P. B. Littlewood, Nature (London) **433**, 607 (2005).
[13] M. J. Calderon, L. Brey, and F. Guinea, Phys. Rev. B **60**, 6698 (1999).
[14] S. W. Jin, X. Y. Zhou, W. B. Wu, C. F. Zhu, H. M. Weng, H. Y. Wang, X. F. Zhang, B. J. Ye, and R. D. Han, J. Phys. D **37**, 1841 (2004).
[15] M. P. de Jong, I. Bergenti, V. A. Dediu, M. Fahlman, M. Marsi, and C. Taliani, Phys. Rev. B **71**, 014434 (2005).
[16] J. Stöhr, *NEXAFS Spectroscopy* (Springer, Berlin, 1992), Vol. 25.
[17] T. Saitoh, A. E. Bocquet, T. Mizokawa, H. Namatame, A. Fujimori, M. Abbate, Y. Takeda, and M. Takano, Phys. Rev. B **51**, 13942 (1995).
[18] J. -H. Park, C. T. Chen, S. -W. Cheong, W. Bao, G. Meigs, V. Chakarian, and Y. U. Idzerda, Phys. Rev. Lett. **76**, 4215 (1996).
[19] K. Horiba, A. Chikamatsu, H. Kumigashira, M. Oshima, N. Nakagawa, M. Lippmaa, K. Ono, M. Kawasaki, and H. Koinuma, Phys. Rev. B **71**, 155420 (2005).
[20] A. Sekiyama, S. Suga, M. Fujikawa, S. Imada, T. Iwasaki, K. Matsuda, T. Matsushita, K. V. Kaznacheyev, A. Fujimori, H. Kuwahara, and Y. Tokura, Phys. Rev. B **59**, 15528 (1999).
[21] R. J. Lad and V. E. Henrich, Phys. Rev. B **38**, 10860 (1988).
[22] M. F. Hundley and J. J. Neumeier, Phys. Rev. B **55**, 11511 (1997).
[23] S. B. Oseroff, M. Torikachvili, J. Singley, S. Ali, S. -W. Cheong, and S. Schultz, Phys. Rev. B **53**, 6521 (1996).
[24] T. A. Tyson, Q. Qian, C. -C. Kao, J. -P. Rueff, F. M. F. de Groot, M. Croft, S. -W. Cheong, M. Greenblatt, and M. A. Subramanian, Phys. Rev. B **60**, 4665 (1999).
[25] T. Friessnegg, S. Madhukar, B. Nielsen, A. R. Moodenbaugh, S. Aggarwal, D. J. Keeble, E. H. Poindexter, P. Mascher, and R. Ramesh, Phys. Rev. B **59**, 13365 (1999).
[26] M. Sirena, N. Haberkorn, M. Granada, L. B. Steren, and J. Guimpel, J. Magn. Magn. Mater. **272-276**, 1171 (2004).
[27] F. M. F. de Groot, J. C. Fuggle, B. T. Thole, and G. A. Sawatzky, Phys. Rev. B **42**, 5459 (1990).
[28] S. P. Cramer, F. M. F. deGroot, Y. Ma, C. T. Chen, F. Sette, C. A. Kipke, D. M. Eichhorn, M. K. Chan, W. H. Armstrong, E. Libby, G. Christou, S. Brooker, V. McKee, O. C. Mullins, and J. C. Fuggle, J. Am. Chem. Soc. **113**, 7937 (1991).